

Experimental and numerical analysis of the behavior of rehabilitated aluminum structures using chopped strand mat GFRP composite patches

Chopped strand
mat GFRP
composite
patches

Sultan Mohammed Althahban

Department of Mechanical Engineering, Jazan University, Jazan, Saudi Arabia

Mostafa Nowier, Islam El-Sagheer and Amr Abd-Elhady

*Mechanical Design Department, Faculty of Engineering, Helwan University,
Cairo, Egypt*

Hossam Sallam

Faculty of Engineering, Zagazig University, Zagazig, Egypt, and

Ramy Reda

*Civil Engineering Department, Higher Technological Institute,
10th of Ramadan, Egypt*

Received 3 March 2024

Revised 26 March 2024

30 March 2024

Accepted 7 April 2024

Abstract

Purpose – This paper comprehensively addresses the influence of chopped strand mat glass fiber-reinforced polymer (GFRP) patch configurations such as geometry, dimensions, position and the number of layers of patches, whether a single or double patch is used and how well debonding the area under the patch improves the strength of the cracked aluminum plates with different crack lengths.

Design/methodology/approach – Single-edge cracked aluminum specimens of 150 mm in length and 50 mm in width were tested using the tensile test. The cracked aluminum specimens were then repaired using GFRP patches with various configurations. A three-dimensional (3D) finite element method (FEM) was adopted to simulate the repaired cracked aluminum plates using composite patches to obtain the stress intensity factor (SIF). The numerical modeling and validation of ABAQUS software and the contour integral method for SIF calculations provide a valuable tool for further investigation and design optimization.

Findings – The width of the GFRP patches affected the efficiency of the rehabilitated cracked aluminum plate. Increasing patch width WP from 5 mm to 15 mm increases the peak load by 9.7 and 17.5%, respectively, if compared with the specimen without the patch. The efficiency of the GFRP patch in reducing the SIF increased as the number of layers increased, i.e. the maximum load was enhanced by 5%.

Originality/value – This study assessed repairing metallic structures using the chopped strand mat GFRP. Furthermore, it demonstrated the superiority of rectangular patches over semicircular ones, along with the benefit of using double patches for out-of-plane bending prevention and it emphasizes the detrimental effect of defects in the bonding area between the patch and the cracked component. This underlines the importance of proper surface preparation and bonding techniques for successful repair.

© Sultan Mohammed Althahban, Mostafa Nowier, Islam El-Sagheer, Amr Abd-Elhady, Hossam Sallam and Ramy Reda. Published in *Frontiers in Engineering and Built Environment*. Published by Emerald Publishing Limited. This article is published under the Creative Commons Attribution (CC BY 4.0) licence. Anyone may reproduce, distribute, translate and create derivative works of this article (for both commercial and non-commercial purposes), subject to full attribution to the original publication and authors. The full terms of this licence may be seen at <http://creativecommons.org/licences/by/4.0/legalcode>

Author's contributions: All authors made equal contributions.

Editor: (Filled by: Journal Staff)



Frontiers in Engineering and Built
Environment

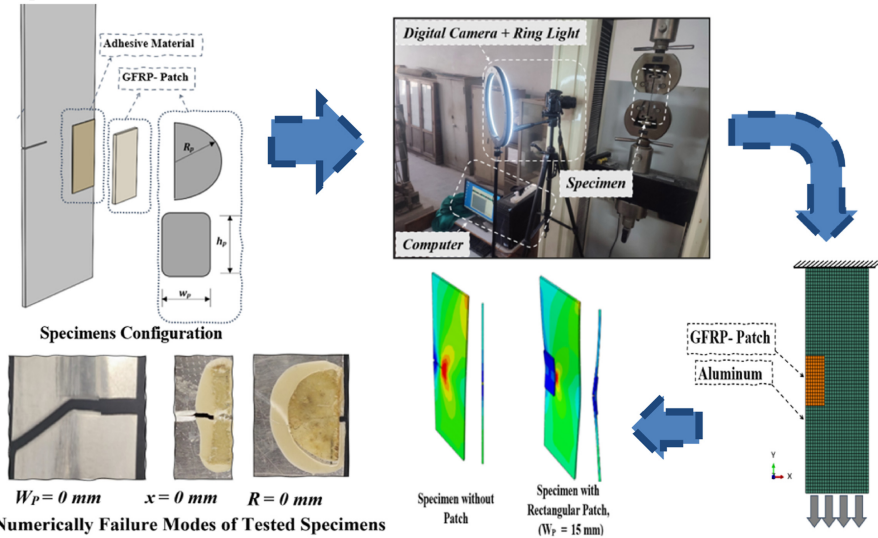
Emerald Publishing Limited

e-ISSN: 2634-2502

p-ISSN: 2634-2499

DOI 10.1108/FEBE-03-2024-0006

Graphical abstract –



Numerically Failure Modes of Tested Specimens

Keywords Composite patches, GFRP, Aluminum elements, Stress intensity factor, FEM

Paper type Research paper

1. Introduction

Rehabilitation or reinforcing the cracked parts of metal elements to restore their efficiency is a crucial concern for military and civilian structures (Schubbe and Mall, 1999; Kumar and Hakeem, 2000; Wang and Pidaparti, 2002; Chung and Yang, 2003). Shaaban and his colleagues examined the capability of fiber-reinforced polymer (FRP) in repairing and strengthening different types of concrete structures (Montaser *et al.*, 2022; Shaaban and Torkey, 2015; Khaleel *et al.*, 2013). Besides, glass fiber-reinforced polymer (GFRP) composites are extensively used because of their desirable qualities, which include low weight, a high strength-to-weight ratio, high stiffness, good dimensional stability and corrosion resistance. Creating glass fibers involves mixing raw materials such as silica or silica-based oxides, melting them in a furnace and extruding the molten glass through fine holes in a platinum or rhodium alloy bushing. The emerging fibers are then consistently drawn to the desired size and cooled or quenched using an air or water jet/spray. A protective chemical coating enhances bonding and safeguards the fiber surfaces. In composite applications, the diameter of glass fibers typically ranges from four to 34 μm . The drawn and sized fibers are collected onto a drum to form a package, which is then dried in an oven and either palletized or further processed into yarn, tow or roving. Glass fibers exhibit lower stiffness, reasonable strength and weight and higher elongation than other types of fibers. Glass fibers are widely employed in the manufacturing of a diverse range of products (Ahmad, 2009; Eqbal *et al.*, 2020).

Composite patches are highly effective for restoring metal and composite components. These patches offer numerous benefits over alternative repair techniques. They enhance fatigue resistance, mitigate corrosion and are simple to shape (Bouiadjra *et al.*, 2003). Notably, composite patches boast the significant advantage of not necessitating the creation of new perforations during installation, thereby preserving structural integrity without compromising strength. Additionally, the thickness required for composite patches ranges from 33% to 50% of that needed for aluminum patches (Günther and Maier, 2010). Okafor

et al. (2005) studied the effectiveness of bonded composite patches in repairing cracked aluminum sheets. They found that the maximum load of the patched specimens was significantly higher than that of the unpatched specimens. *Madani et al.* (2009) numerically studied the effects of using single and double-sided composite patches to decrease the stress concentration at notches. They found that using a double-sided patch was more effective in bending due to the eccentricity of the one-sided patch and reduced the shear stresses in the adhesive. Adhesively bonded composite repairs increase the fatigue life of broken components in aircraft construction because they offer several benefits, including a high strength-to-weight ratio, fatigue resistance and corrosion resistance (*Madani et al.*, 2009; *Ramji and Srilakshmi*, 2012). *Ouinan et al.* (2007a, b) applied the finite element method (FEM) to analyze the crack growth behavior of a semicircular notch repaired by a boron/epoxy composite patch. They found that increasing the semicircular patch radius decreases the stress concentration and the stress intensity factor (SIF).

Moreover, the influence of patch shape (circular, rectangular, trapezoid and elliptical) for carbon-epoxy and boron-epoxy patches and their mechanical properties on the SIF of the cracked plate was numerically studied (*Kaddouri et al.*, 2008; *Sadek et al.*, 2018; *Hosseini-Toudeshky et al.*, 2013). Additionally, several researchers had previously evaluated the effects of fully bonded (*El-Emam et al.*, 2016, 2017; *Khan and Essaheb*, 2017; *Abd-Elhady et al.*, 2017, 2020), partially bonded (*Albedah et al.*, 2018a, b; *Bellali et al.*, 2021) and welded patches (*Abd-Elhady*, 2013). *Albedah et al.* (2018a, b) studied the effect of patch length on one-side bonded composite patches for aluminum panels. *Makwana et al.* (2018) compared symmetric and asymmetric composite patches. They discovered that symmetric patches reduce the stress in a cracked aluminum plate more effectively than asymmetric patches, resulting in a more significant SIF reduction. (*Makwana et al.*, 2018; *Deghoul et al.*, 2019) studied the effects of the crack inclination and the patch shape on the repaired aluminum plates under fatigue. They observed that the crack inclination considerably affects the aluminum plates' fatigue life and the patch shape highly affects the repaired plate's fatigue life. Furthermore, the contour integral method (CIM) has been implemented in many studies. *El-Sagheer et al.* (2020) used CIM to investigate the influence of composite patches on restoring cracked metal plates. Fatigue experiments were carried out on V-notch cracked specimens utilizing two aluminum alloys (2024-T3 and 7075-T6) repaired with bonded carbon/epoxy patches under continuous amplitude loading with a positive stress ratio. Rectangular, trapezoidal and triangular composite patch forms were employed. In this study, the patch shape significantly affects the performance of bonded composite repairs in aircraft structures (*Mohammed et al.*, 2021). *Mohammadi* (2020) numerically studied how several characteristics, such as the thickness of a fractured plate, affected the performance and longevity of a one-sided composite patch mending procedure. The results revealed that the influence of various factors on the efficiency and durability of a one-sided patch depended on the thickness of the repaired plate and the thickness and substance of the patch. *Li et al.* (2019) investigated the influence of patch form by bonding single- and double-sided exterior patches. The effectiveness of various patch forms was investigated using ultimate tensile strength, stress concentration factor and peel stress, and it was observed that the square patch performs better than other patches. *Matta et al.* (2019) investigated the in-plane compression behavior of open-hole carbon fiber composite specimens connected to external carbon fiber composite patches. In the case of patch-bonded carbon fiber composite specimens, the failure mechanism starts with partial patch debonding, followed by complete specimen failure.

2. Research significant

Repairing metallic structures using uniaxial or cross-ply laminated composite materials has been extensively used. However, research on repairing metallic structures using the chopped

strand mat GFRP has been relatively limited, thus creating a critical gap in the literature. This paper comprehensively addresses this gap by examining the influence of chopped strand mat GFRP patch configurations such as patch geometry, patch dimensions, patch position, the number of patch layers, whether a single or double patch is used and how well debonding the area under the patch improves the strength of the cracked aluminum plates with different crack lengths. Furthermore, a three-dimensional (3D) FEM was adopted to simulate the repaired cracked aluminum plates using composite patches to obtain the SIF using the CIM for the various patch configurations. The numerical modeling and validation of ABAQUS software and the contour integral method for SIF calculations provide a valuable tool for further investigation and design optimization. This approach allows for virtual testing and reduces the need for extensive experimental samples.

3. Experimental program

3.1 Material properties

About 1,050 aluminum plates of 150 mm in length and 50 mm in width were used. The chemical composition and mechanical properties of 1,050 aluminum plates are listed in [Tables 1 and 2](#). GFRP composites as patch materials were used in the current study. The patches consisted of one layer (0.25 mm in thickness) or two layers (0.5 mm in thickness) that were bonded together on one (single) or both (double) sides of the aluminum plate. A hand lay-up approach was employed using chopped strand mat glass fiber of 13 μm in diameter supplied by JMS (Chongqing, China), polyester of 37.4% solvent content and density of (1.11 g/cm^3) was used as a matrix, and the polyester was fully hardened after six hours. However, the adhesive material was epoxy (Kemapoxy-165G) of 0.1 mm in thickness with a resin-to-hardener ratio of 8:1; the epoxy density was (1.12 g/cm^3); the epoxy was strongly resistant to mechanical stresses and chemical effects and fully hardened after seven days. The polyester and epoxy were supplied by CMB (Giza, Egypt). [Table 3](#) explains the mechanical properties of the composite patches used in this study: fibers, polyester and epoxy. [Figure 1](#) shows the stress–strain curve of the present patch.

Table 1.
The chemical composition of 1,050 aluminum plates

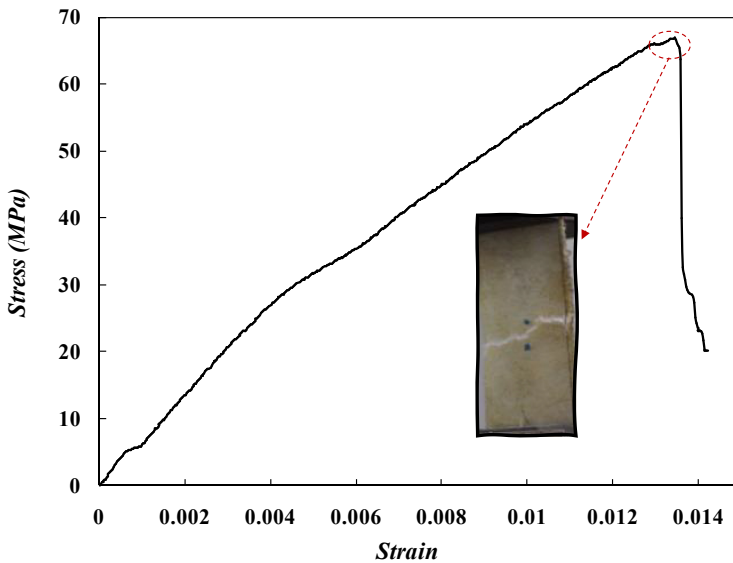
DIN marking	Si	Fe	Cu	Mn	Mg	Cr	Zn	Ti	V	Other each
Al 99.5	0.25	0.40	0.05	0.05	0.05	0.05	0.05	0.03	0.05	0.03

Table 2.
The mechanical properties of 1,050 aluminum plates

Yield stress (MPa)	UTS (MPa)	E (GPa)	G (GPa)	N	Elongation%
25	75	70	26.32	0.33	37%

Table 3.
The mechanical properties of the matrix and fiber

Material	E (GPa)	G (GPa)	ν
E-glass fiber	82	30.13	0.2
Polyester	4.8	1.19	0.3
Epoxy	3.24	1.8	0.36



Chopped strand
mat GFRP
composite
patches



Figure 1.
Stress–strain curve of
the patch

3.2 Specimen preparation and test setup

Single-edge cracked aluminum specimens of 150 mm in length and 50 mm in width were tested using the tensile test. The crack was oriented perpendicularly to the specimen's height with ($a/W = 0.2, 0.3$ and 0.6) using a low-speed saw, as shown in [Figure 2](#).

The cracked aluminum specimens were then repaired using GFRP patches with various configurations. As mentioned before, epoxy was used to attach the patches to the cracked aluminum specimens. The specimen dimensions and configurations of the patches were placed in [Table 4](#). [Figure 3](#) shows the test setup. A 300-kN universal testing machine with a

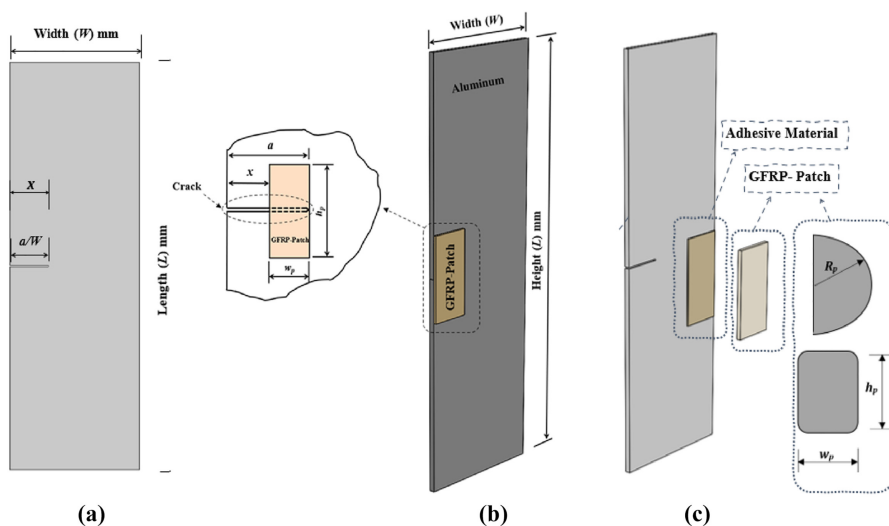


Figure 2.
Illustrations of test
specimen with patch:
(a) The assembly of the
patch on the specimen,
(b) Exploded view of
the patch, adhesive
material and the
specimen and (c)
Specimen
configuration

FEBE

2 mm/min loading rate controlled by uniform axial displacement was used. Five specimens for each case were tested to failure to validate the results.

4. Finite element model

A 3D FEM using ABAQUS was performed to study the effectiveness of repairing patches on single-edged cracked aluminum specimen plates and to predict the SIF (ABAQUS, 2014).

4.1 Geometry and mechanical properties

The geometries of the patches and aluminum specimens are shown in Figure 1. The mechanical properties of the GFRP patch are listed in Table 5 and obtained from the following equations (Campbell, 2010):

Table 4.
Specimens dimensions and configurations of the patches

Parameter	Value
The aluminum specimen height (L), mm	150
The aluminum specimen width (W), mm	50
The aluminum specimen thickness (t), mm	2
Crack length (a)	(0.2, 0.3 and 0.6) W
The position of the patch (x)	(0, 0.1, 0.3 and 0.6) W
Patch width (w_p), mm	5, 15 and 30
Patch height (h_p), mm	30
Equivalent patch radius (R_p), mm	10, 17 and 24
Number of patch layers (N)	One, two
Debonding area/total patch area (A)	($\frac{1}{3}$, $\frac{1}{2}$ and $\frac{2}{3}$)

Figure 3.
Test setup

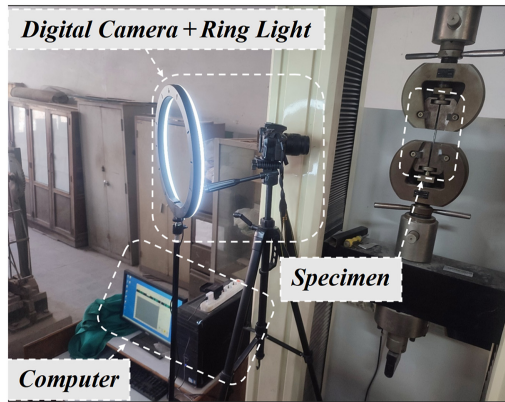


Table 5.
Mechanical properties of the patch

Material	E_{Random} (GPa)	G_{Random} (GPa)	ν_{Random}	L_f (mm)	d_f (μm)
GFRP patch	11.2	3.9	0.41	30	13

$$\mathbf{E}_{11} = \frac{1 + 2\left(\frac{L_f}{d_f}\right)\eta_L V_f}{1 - \eta_L V_f} \mathbf{E}_m \quad (1)$$

$$\mathbf{E}_{22} = \frac{1 + 2\eta_T V_f}{1 - \eta_T V_f} \mathbf{E}_m \quad (2)$$

$$\eta_L = \frac{\left(\frac{E_f}{E_m}\right) - 1}{\left(\frac{E_f}{E_m}\right) + 2\left(\frac{L_f}{d_f}\right)} \quad (3)$$

$$\eta_T = \frac{\left(\frac{E_f}{E_m}\right) - 1}{\left(\frac{E_f}{E_m}\right) + 2} \quad (4)$$

$$\mathbf{E}_{Random} = \frac{3}{8}\mathbf{E}_{11} + \frac{5}{8}\mathbf{E}_{22} \quad (5)$$

$$\mathbf{G}_{Random} = \frac{1}{8}\mathbf{E}_{11} + \frac{1}{4}\mathbf{E}_{22} \quad (6)$$

$$\nu_{Random} = \frac{\mathbf{E}_{Random}}{2\mathbf{G}_{Random}} - 1 \quad (7)$$

For the mechanical properties of fibers and matrix (polyester), f refers to fiber and m refers to matrix. In addition, E is the elastic modulus, G is the shear modulus, ν is the Poisson's ratio, V_f is the fiber volume fraction, L_f is the fiber's length, d_f is the fiber's diameter and η_T and η_L are constants. On the other hand, the mechanical properties of the GFRP patch were as follows: E_{11} is the longitudinal elastic modulus and E_{22} is the transverse elastic modulus. E_{Random} is the random elastic modulus, G_{Random} is the random shear modulus and ν_{Random} is the random Poisson's ratio.

4.2 Boundary condition and loading step

Constant axial displacement control was applied to the specimens. The specimens' boundary conditions are shown in Figure 4. The specimens were placed between two grips; the upper grip was fixed and the lower grip was free to move vertically with displacement control. The composite layers were connected using the tie contact feature available in ABAQUS/Standard.

4.3 Contact and mesh generation

Eight-node linear brick (C3D8R) was corroborated with the contour integral and was used to mesh all model elements, as shown in Figure 4.

5. Results and discussion

5.1 Effect of patch width (W_p)

Figure 5 shows the effect of patch width W_p ; 0, 5, 15 and 30 mm on the peak load (failure load) of the tested specimens with $a = 0.3 W$, i.e. $a = 15$ mm and $x = 0$. Increasing patch width up to

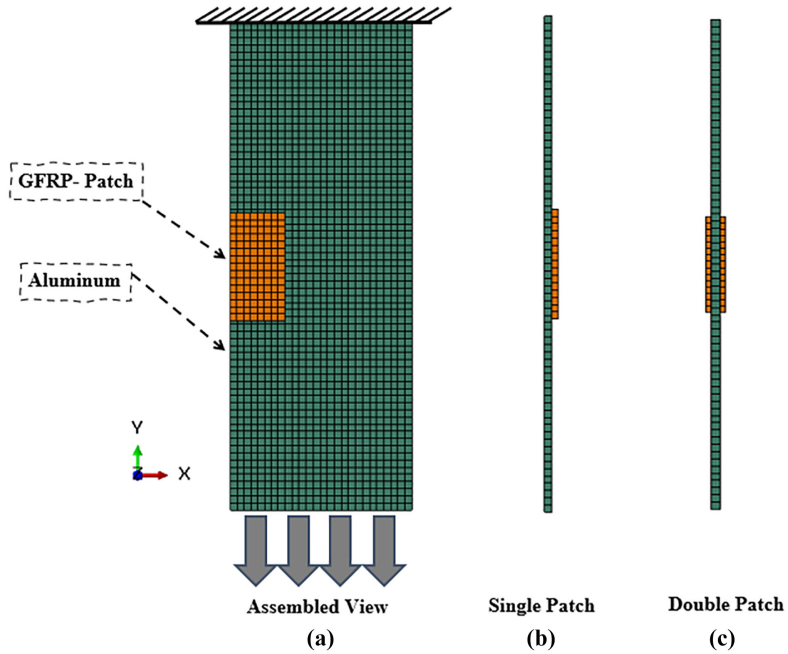


Figure 4.
Meshing of the model

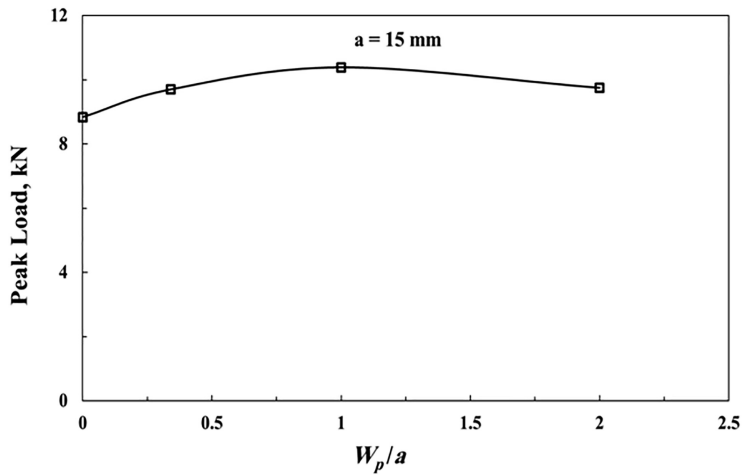


Figure 5.
Effect of the
patch width

15 mm ($W_p/a = 1$) increases the resistance to crack propagation, i.e. increasing the peak load to failure. Patch width might influence how effectively stress is distributed around the crack. Patch width W_p equals 15 mm, which might offer a larger area for stress to dissipate, leading to a more apparent benefit than patch width W_p equals 5 mm. The cracked aluminum specimen without patch width $w_p = 0$ mm gives a failure load of 8.84 kN, while the failure load of the cracked aluminum specimen with patch width $w_p = 15$ mm was 10.39 kN, which

indicates that the ultimate load of the unstrengthened specimen increased by about 17.5%. However, the specimen with patch width $w_p = 30$ mm had a maximum load of 9.75 kN and the failure load of the specimen with patch width $w_p = 5$ mm was 9.7 kN. Figure 6 shows the failure mode of the tested specimens. Increasing patch width W_p from 5 mm to 15 mm increases the peak load by 9.7 and 17.5%, respectively, if compared with the specimen without the patch. Similar results were reported in (Albedah *et al.*, 2018a, b; Abd-Elhady *et al.*, 2020; Shahin and Farid, 2017). It can be concluded that the patch width $w_p = 15$ mm ($W_p/a = 1$) gives the highest enhancement to crack propagation resistance, as it covers 100% of the crack length and narrow region of the crack tip. In contrast, the patch ($w_p = 30$ mm) shows a lower value than the patch ($w_p = 15$ mm) because it faces a large region with maximum stress around the crack tip.

5.2 Effect of patch shape

A comparison between the effect of patch shape, either rectangular or semicircular, on the failure load of the cracked aluminum specimen with $a = 0.3 W$ (where $x = 0$) was conducted and shown in Figure 7. Three different radii for semicircular patches of 10, 17 and 24 mm were chosen to be equivalent in area to the rectangular patches of 5×30 , 15×30 and 30×30 mm, respectively, as shown in the figure. The same trend was obtained for semicircular patches;

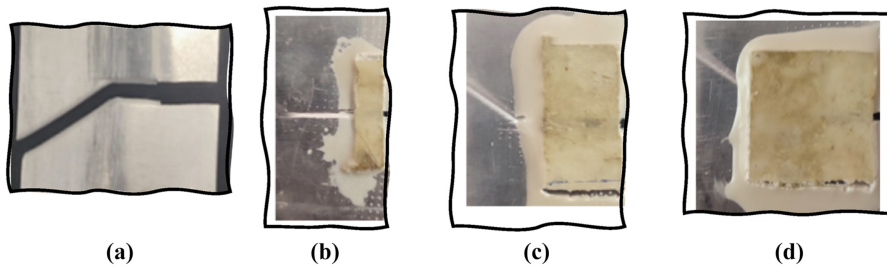


Figure 6.
Effect of the patch width on failure mode:
(a) $W_p = 0$ mm, (b) $W_p = 5$ mm, (c) $W_p = 15$ mm and (d) $W_p = 30$ mm

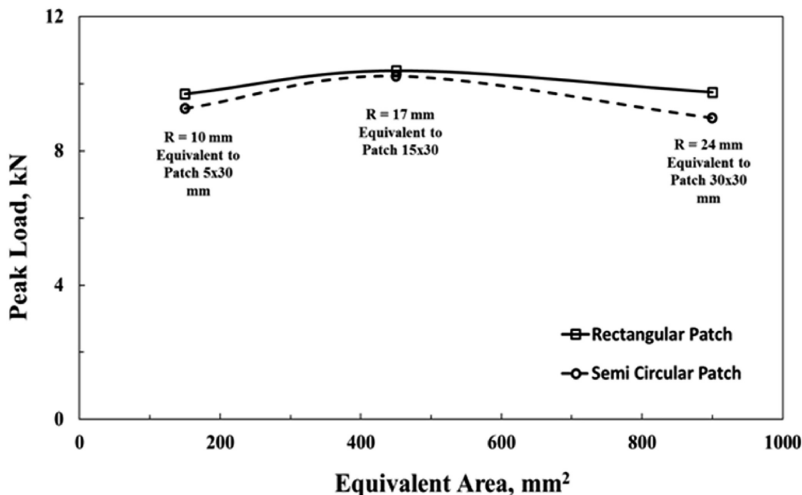


Figure 7.
Peak load as a function of the patch shape

increasing the patch radius from 10 mm to 17 mm increased the peak load by 10.4%, but the peak load decreased by 3% when using a semicircular patch with a radius of 24 mm.

A semicircular patch with a radius of 10 mm gives a peak load of 9.27 kN less than the equivalent rectangular patch of 5×30 mm, which gives 9.7 kN with a decrease of 4.6% in peak load and a semicircular patch with a radius of 17 mm provides a peak with a load so close to the equivalent rectangular patch of 15×30 mm with a difference of 1.5%. Finally, a semicircular patch with a radius of 24 mm gives a peak load of 8.9 kN less than the equivalent rectangle patch of 5×30 mm, which gives 9.75 kN with a decrease of 8.5% in peak load. [Figure 8](#) shows the tested specimens repaired with semicircular patches. As mentioned, the rectangular patch is more efficient than the semicircular patch. This may be because area 2 in the rectangular patches with well-defined edges demonstrates superior performance in suppressing crack propagation compared to area 1 in the semicircular patches with the equivalent area. This area could be more efficient in suppressing both in-plane and out-of-plane bending stresses around the crack tip. Area 1 in the semicircular patches might contribute to capturing crack openings.

5.3 Effect of single or double patch

Single and double (on both sides of specimens) rectangular patches were used to repair the 15 mm crack length for three cases of W_p : 5 mm, 15 mm and 30 mm, as illustrated in [Figure 9](#). The peak loads for single patch widths 5, 15 and 30 mm were 9.7, 10.39 and 9.75 kN, respectively. On the other hand, the peak loads for double patches with width 5, 15 and 30 mm were 11.25, 10.45 and 10.24 kN, respectively.

As observed, double patches reduce part of the damage due to out-of-plane bending and restrict crack growth to enhance the peak load. The load enhancement was 16, 0.6 and 5.0% for W_p 5, 15 and 30 mm, respectively. This agrees with the results obtained by [Abd-Elhady et al. \(2020\)](#) and [Abdelmoumin et al. \(2023\)](#). A double patch with W_p equal to 15 mm gives a peak load close to that of a single patch for the same width, with an increase of only 0.6%. This means that using a single patch with W_p equal to the crack length, a , was so effective that it was enough to enhance the peak load. Double patches are generally preferred because they reduce out-of-plane bending and increase the peak load. Double patches typically provide superior repair compared to single patches for crack repair. Their ability to mitigate out-of-plane bending stresses leads to a higher load capacity. However, for crack lengths similar to the patch width, a single, well-sized patch might be a viable and more economical option. Additionally, the difference between single and double patches is confined by a closed

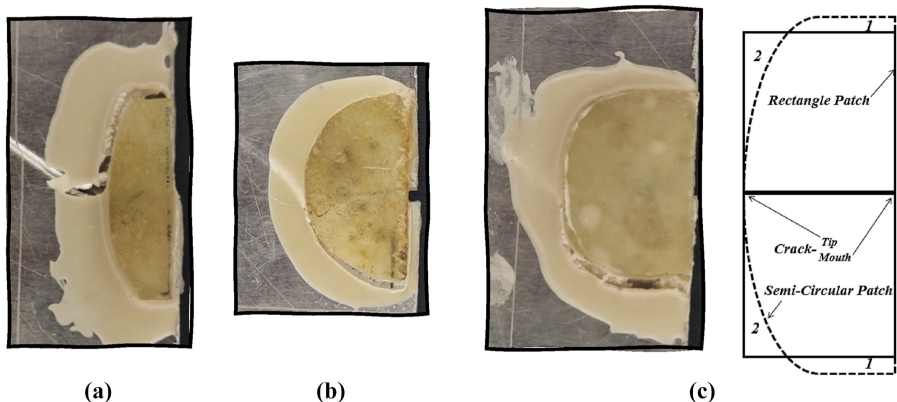
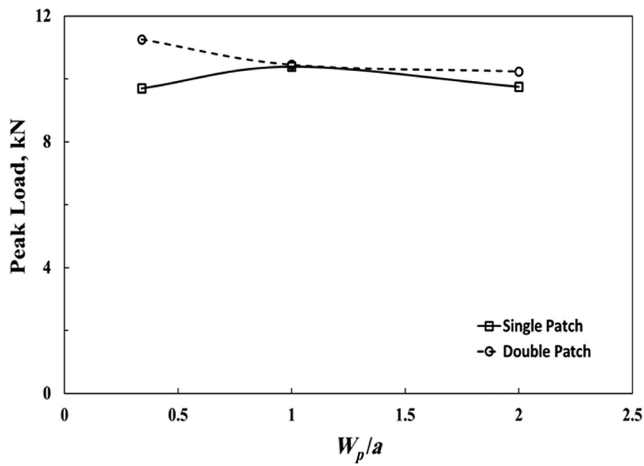


Figure 8.
Effect of the patch shape on failure mode:
(a) $R = 10$ mm, (b) $R = 17$ mm and
(c) $R = 24$ mm



Chopped strand
mat GFRP
composite
patches

Figure 9.
The single and double
patch effectiveness

value beyond ($W_p = 15$ mm) because the extra area – in single patches – which covers the uncracked zone can reduce out-of-plane bending.

5.4 Effect of patch position

Figure 10 shows the effect of patch position with W_p equal to 5 mm on repairing aluminum cracked specimens (with $a/W = 0.3$) to obtain the most suitable position. As shown in the figure, applying the patch directly at the crack tip ($x = 0$ mm) successfully restrains the crack mouth opening displacement (CMOD) and increases the failure load, which gives the best enhancement when compared to two other patch positions, $x = 5$ and $x = 15$ mm. The peak load of the patch affixed at $x = 0$ mm was 9.85 kN, with increases of 13.8 and 1.5% when compared with $x = 5$ and 15 mm, respectively. However, using the patch at $x = 5$ mm fails to sustain the crack opening for the cracked aluminum specimen and decreases the peak load by 13.8 and 12.4% when compared with $x = 0$ and 15 mm. Abd-Elhady (2013) obtained similar results. It can be concluded that positioning the patch directly on the crack surface provides immediate support and restricts the initial stages of crack opening. This significantly reduces

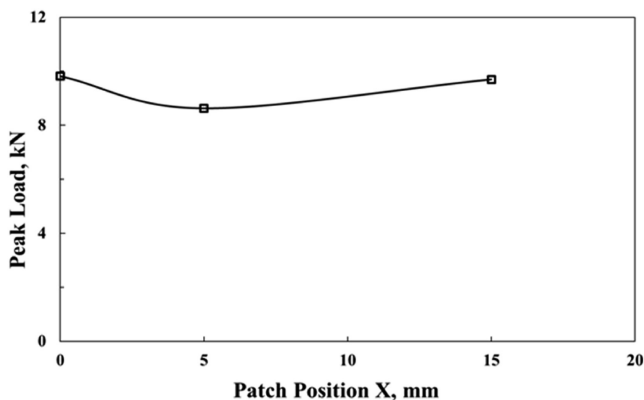


Figure 10.
Effect of patch position

stress concentration at the crack's leading edge, delaying crack propagation and ultimately increasing the overall load capacity of the specimen. The failure behavior of the tested specimens with different patch positions is shown in [Figure 11](#).

5.5 Effect of patch layers number

One and two layers for single patches of width w_p equal to 5, 15 and 30 mm were tested (where $a/W = 0.3$), and their results are shown in [Figure 12](#). It is clear from the figure that two-layer patches of width ($w_p = 5$ and 30 mm) were more effective in resisting crack growth and yielded higher load compared to one-layer patches; the failure load were 10.19 and 10.21 kN, respectively, with increases of 5 and 4.7% when compared to one layer patches, which yielded 9.7 and 9.75 kN, respectively. However, the failure load of two-layer patches of width ($w_p = 15$ mm) was very close to that of one-layer patches of width ($w_p = 15$ mm). Hence, the adhesive material (polyester) between the two-layer patch begins to fail before the adhesive material (epoxy) between the patch and the aluminum plate. It can be noted that using patches with two layers was more effective for repairing cracked aluminum plates, which led to an increase in the peak load and resistance the crack growth, the same observation obtained by [Abd-Elhady et al. \(2020\)](#) and [Abdelmoumin et al. \(2023\)](#).

Figure 11.
Effect of the patch position on failure mode: (a) $x = 0$ mm, (b) $x = 5$ mm and (c) $x = 15$ mm

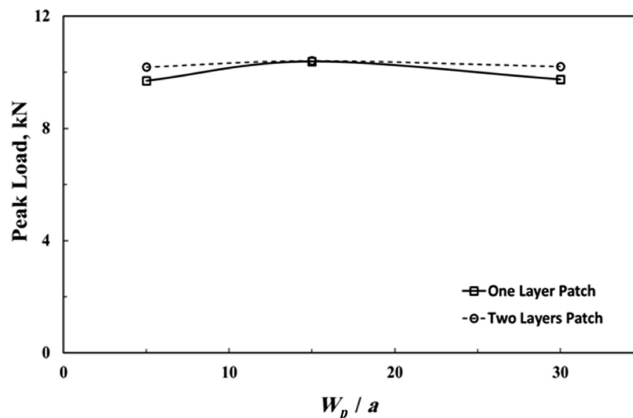
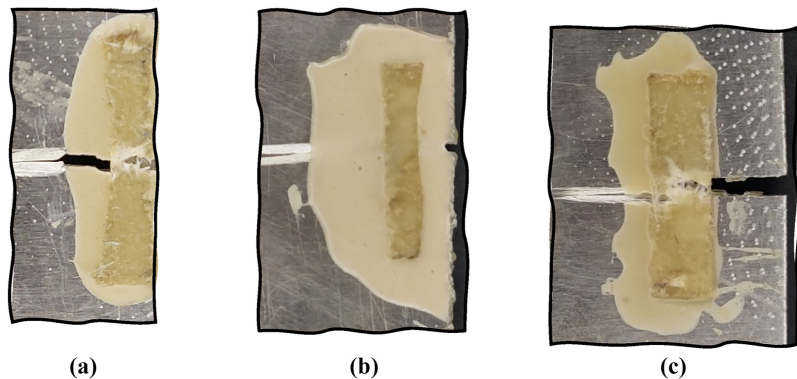


Figure 12.
Peak load as a function of the patch layers number

5.6 Effect of crack length

The effect of crack lengths 10, 15 and 30 mm was studied and shown in Figure 13. As expected, increasing the crack length decreases the failure load because cracks act as stress concentrators, so increasing the crack length reduces applied loads and leads to earlier failure. For cracked specimens without patches, the failure loads decreased by 17 and 52.5% for specimens with 15 and 30 mm crack lengths, respectively, if compared with specimens without patches and crack lengths of 10 mm. The same observation was held for single and double patches, with peak loads for single patches of 15 and 30 mm crack length decreasing by 5.5 and 49.7%, respectively, if compared with a specimen with a single patch on a 10 mm crack length. The failure loads for double patches of 15 and 30 mm crack length decreased by 5.8 and 46.9%, respectively, if compared with a specimen with double patches of 10 mm crack length. These results agree with those reported by Kumar and Hakeem (2000), Chung and Yang (2003), Khan and Essaheb (2017) and Albedah *et al.* (2018a, b).

The enhancement in the failure loads of the repaired specimens using the patches (single or double) was very clear, as seen in the figure, when compared with the specimens without patches. On the other hand, only a slight change was noted when using a double patch compared to a single patch. The effect of single and double patches was apparent when W_p equals 5 and 30 mm but was found to be ineffective when W_p equals 15 mm (current state).

5.7 Effect of imperfection distance

Various external factors may influence the bonding process between patches and the surface of the cracked specimens. Therefore, it was helpful to create an isolating region between patches (where $w_p = 15$ mm) and cracked specimens to study the effect of the debonding region and its areas on the failure load. The isolating region (debonding region) in this study was supposed to be ($\frac{1}{3}$, $\frac{1}{2}$ and $\frac{2}{3}$) of the total area of the adhesive layer. As expected, increasing the debonding area decreases the failure load, as shown in Figure 14.

In the first case (the debonding area was $\frac{1}{3}$ of the total area), the specimens give a 9.83 kN failure load with a decrease of 5.7% compared to the tested specimen with a full patch area bond, which provides a failure with a load of 10.39 kN. Using a debonding area of $\frac{1}{2}$ and $\frac{2}{3}$ of the total area gives the same failure load with a decrease of 16% if compared with the tested specimen that has a full patch area bond, and this value is very close to the failure of the tested specimen without a patch. As mentioned, the debonding area of $\frac{1}{2}$ and $\frac{2}{3}$ when compared to the

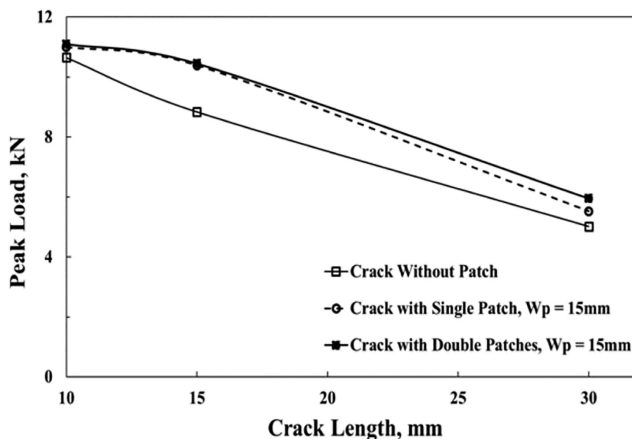


Figure 13.
Effect of crack length

FEBE

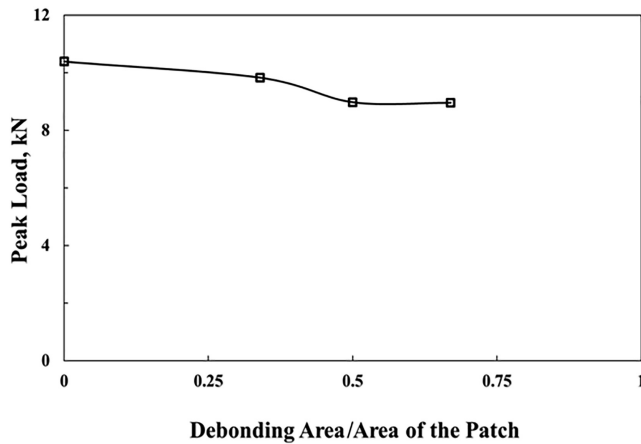


Figure 14.
Debonding effect of the patch

total area, was inadequate to resist crack growth and increase the failure load if compared with the tested specimen that does not have a patch, which gives a failure load of 8.84 kN. Therefore, treating the specimen surface with patches before repairing it is necessary. [Figure 15](#) shows the cases for when repairs are made.

5.8 Numerical results

From the main parameters that determine the effectiveness of the patch in repairing the cracked structure, it is helpful to reduce the driving force of this crack. Therefore, the Mode I SIF of the cracked aluminum specimen was determined both with and without the patch. The mode I SIF was calculated using CIM. The effect of many parameters on the normalized SIF that was obtained by dividing the Mode I SIF values of the repaired cracked specimens with patches yielding the Mode I SIF values of unrepaired cracked specimens was studied. [Figure 16](#) shows the experimental failure modes of some tested specimens and the numerical simulation of these tests to determine the Mode I SIF.

[Figure 17](#) shows the effect of patch width or radius (for rectangular or semicircular patches, respectively), the number of layers, and the patch type, i.e. single or double, on Mode I, SIF. As seen in [Figure 17\(a\)](#), the patch width, up to 15 mm, showed a decrease in the SIF,

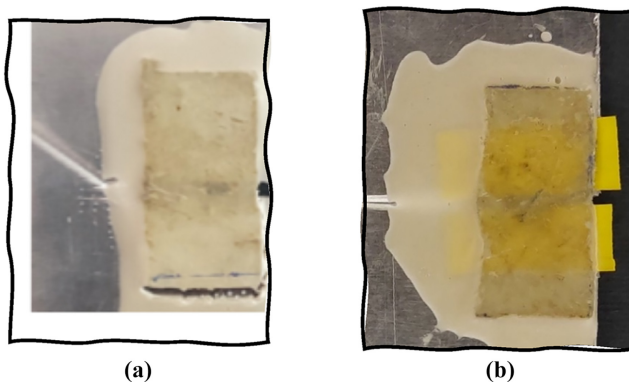


Figure 15.
Effect of the debonding area on failure mode: (a) full bond and (b) $\frac{2}{3}$ of the patch area

which means that increasing the patch width has a positive effect up to 15 mm. After that, the SIF remained almost constant. On the other hand, using double patches reduced the Mode I SIF and subsequently had a more significant effect than using the single patch, but using two layers did not lead to a substantial reduction of the Mode I SIF and, therefore, the efficiency of the repairs.

A similar observation is made from Figure 17(b) for semicircular patches, SIF enhanced, when a radius of 17 mm (equivalent in area to patch width of 15 mm) was used; double patches improve the SIF more than single patches, with only a small effect observed when increasing the patch layer number from one layer to two layers. The effect of crack length (a/W) for a rectangular patch of 15 mm in width with one and two patch layers and a single patch

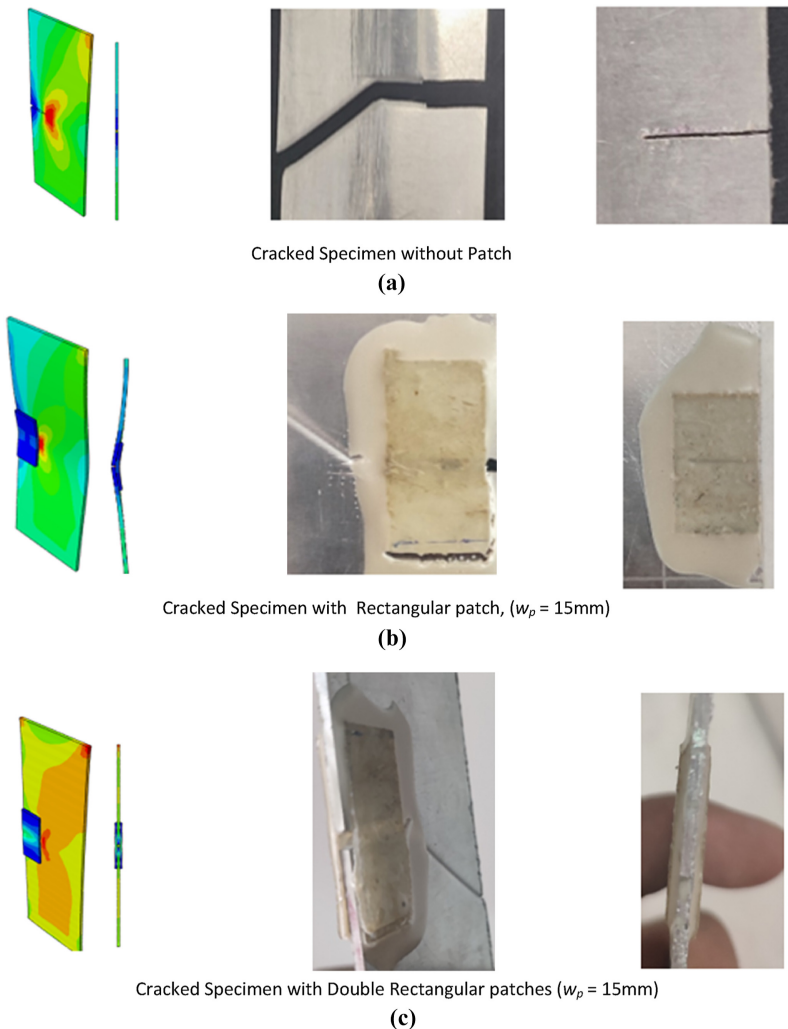


Figure 16.
Numerically and
experimentally failure
modes of tested
specimens

(continued)

FEBE



Cracked Specimen with Semicircular patch ($R_p = 17\text{mm}$)

(d)



Cracked Specimen with Rectangular patch, ($w_p = 5\text{mm}$) at position, ($x = 0$)

(e)

Figure 16.

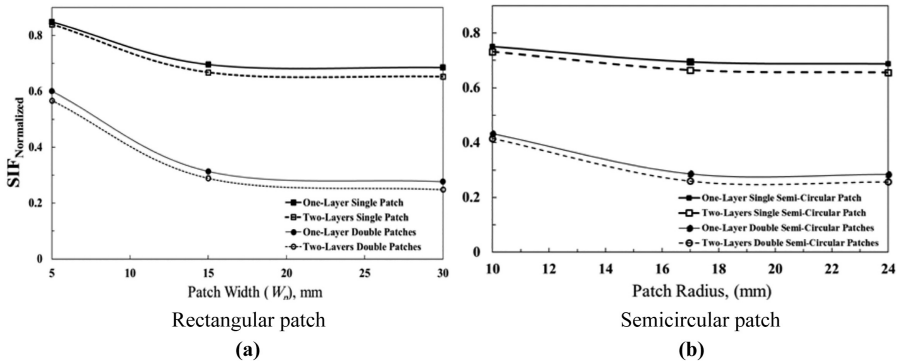


Figure 17.
Effect of the patch (width/radius), layers number and patch type (single or double) on SIF

or double patch on Mode I SIF is shown in Figure 18. The same behavior occurs when using double patches compared with a single patch.

The effect of patch position for a rectangular patch with a crack length (a/W) equal to 0.3 and a patch width of 15 mm on the Mode I SIF was studied and shown in Figure 19(a). Increasing the distance between the crack mouth and the patch edge, x increases the Mode I SIF of the tested specimens, which means the patching efficacy decreased. The most effective patch position was obtained when the patch was placed at location x equals 0.

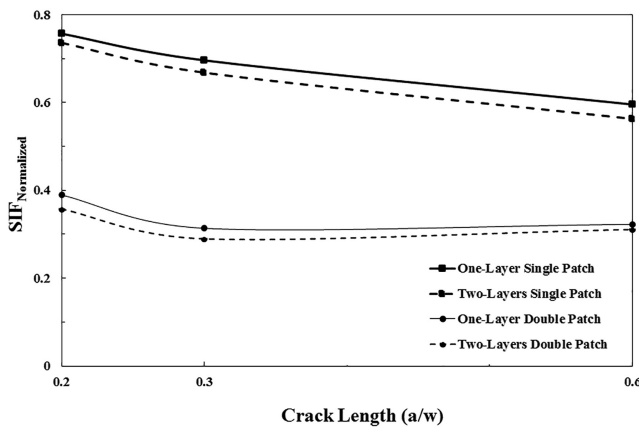


Figure 18.
Effect of the crack length (a/W), number of layers and single or double patch on SIF

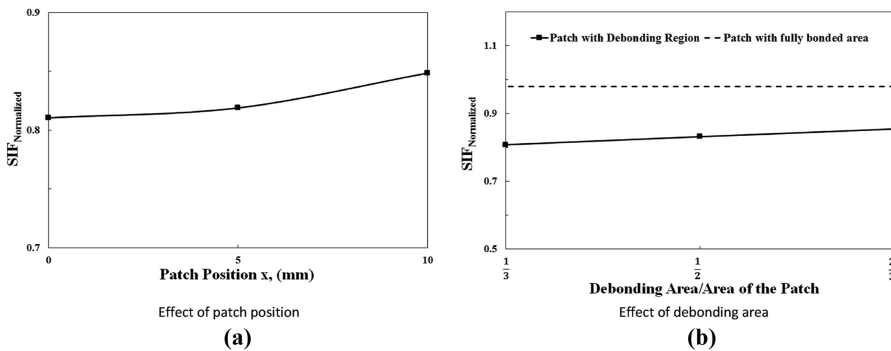


Figure 19.
Effect of (a) the patch position and (b) the debonding area on the mode I SIF

Figure 19(b) shows the effect of the debonding area for a rectangular patch with a crack length (a/W) equal to 0.3 and a patch width of 15 mm on the SIF; increasing the debonding size under the patch leads to an increase in the SIF, which means a decrease in the efficacy of the patches.

6. Conclusions

The numerical and experimental results of the present research indicate the following conclusions can be drawn:

- (1) The width of the GFRP patches affected the efficiency of the rehabilitated cracked aluminum plate. Increasing patch width W_p from 5 mm to 15 mm increases the peak load by 9.7 and 17.5%, respectively, if compared with the specimen without the patch.
- (2) The efficiency of the GFRP patch in reducing the SIF increased as the number of layers increased, i.e. the maximum load was enhanced by 5%.
- (3) The shape of the GFRP patch in the same area considerably affects the efficiency of the rehabilitated cracked plate and reduces the SIF value. The rectangular patch is more efficient than the semicircular patch in reducing the load and SIF.

- (4) Using a double patch improved the composite patch's ability to prevent crack propagation and also prevented out-of-plane bending. Furthermore, the double patches (with either single or double layers) reduce the SIF by half when compared to the single patch.

References

- Abd-Elhady, A.A. (2013), "Effect of location and dimensions of welded cover plate on stress intensity factors of cracked plates", *Ain Shams Engineering Journal*, Dec 1, Vol. 4 No. 4, pp. 863-867, doi: [10.1016/j.asej.2013.03.002](https://doi.org/10.1016/j.asej.2013.03.002).
- Abd-Elhady, A.A., Sallam, H.E. and Mubarak, M.A. (2017), "Failure analysis of composite repaired pipelines with an inclined crack under static internal pressure", *Procedia Structural Integrity*, Jan 1, Vol. 5, pp. 123-130, doi: [10.1016/j.prostr.2017.07.077](https://doi.org/10.1016/j.prostr.2017.07.077).
- Abd-Elhady, A.A., Sallam, H.E., Alarifi, I.M., Malik, R.A. and El-Bagory, T.M. (2020), "Investigation of fatigue crack propagation in steel pipeline repaired by glass fiber reinforced polymer", *Composite Structures*, Jun 15, Vol. 242, 112189, doi: [10.1016/j.compstruct.2020.112189](https://doi.org/10.1016/j.compstruct.2020.112189).
- Abdelmoumin, O.B., Idir, B., Samir, K., Coung, T., Seyedali, M. and Magd, A.M. (2023), "Strength prediction of a steel pipe having a hemi-ellipsoidal corrosion defect repaired by GFRP composite patch using artificial neural network", *Composite Structures*, Vol. 304, 116299, doi: [10.1016/j.compstruct.2022.116299](https://doi.org/10.1016/j.compstruct.2022.116299).
- Ahmad, J. (2009), "Introduction to polymer composites", in *Machining of Polymer Composites*, Springer, New York, NY, pp. 1-35.
- Albedah, A., Bouiadjra, B.B., Benyahia, F. and Mohammed, S.M. (2018a), "Effects of adhesive disbond and thermal residual stresses on the fatigue life of cracked 2024-T3 aluminum panels repaired with a composite patch", *International Journal of Adhesion and Adhesives*, Dec 1, Vol. 87, pp. 22-30, doi: [10.1016/j.ijadhadh.2018.09.004](https://doi.org/10.1016/j.ijadhadh.2018.09.004).
- Albedah, A., Mohammed, S.M. and Bouiadjra, B.B. (2018b), "Bouiadjra BA, Benyahia F. Effect of the patch length on the effectiveness of one-sided bonded composite repair for aluminum panels", *International Journal of Adhesion and Adhesives*, Mar 1, Vol. 81, pp. 83-89, doi: [10.1016/j.ijadhadh.2017.11.012](https://doi.org/10.1016/j.ijadhadh.2017.11.012).
- Bellali, M.A., Serier, B. and Mokhtari, M. (2021), "Campilho RD, Lebon F, Fekirini H. XFEM and CZM modeling to predict the repair damage by composite patch of aircraft structures: debonding parameters", *Composite Structures*, Jun 15, Vol. 266, 113805, doi: [10.1016/j.compstruct.2021.113805](https://doi.org/10.1016/j.compstruct.2021.113805).
- Bouiadjra, B.B., Belhouari, M. and Serier, B. (2003), "Computation of the stress intensity factors for repaired cracks with bonded composite patch in mode I and mixed mode", *Composite Structures*, Vol. 59, pp. 415-418.
- Campbell, F.C. (2010), *Structural Composite Materials*, ASM International, .
- Chung, K.H. and Yang, W.H. (2003), "A study on the fatigue crack growth behavior of thick aluminum panels repaired with a composite patch", *Composite Structures*, Apr 1, Vol. 60 No. 1, pp. 1-7, doi: [10.1016/s0263-8223\(02\)00338-0](https://doi.org/10.1016/s0263-8223(02)00338-0).
- Deghoul, N., Errouane, H., Sereir, Z., Chateaufneuf, A. and Amziane, S. (2019), "Effect of temperature on the probability and cost analysis of mixed-mode fatigue crack propagation in patched aluminium plate", *International Journal of Adhesion and Adhesives*, Oct 1, Vol. 94, pp. 53-63, doi: [10.1016/j.ijadhadh.2019.05.004](https://doi.org/10.1016/j.ijadhadh.2019.05.004).
- El-Emam, H.M., Salim, H.A. and Sallam, H.E. (2016), "Composite patch configuration and prestraining effect on crack tip deformation and plastic zone for inclined cracks", *Journal of Composites for Construction*, Aug 1, Vol. 20 No. 4, 04016002, doi: [10.1061/\(asce\)cc.1943-5614.0000655](https://doi.org/10.1061/(asce)cc.1943-5614.0000655).
- El-Emam, H.M., Salim, H.A. and Sallam, H.E. (2017), "Composite patch configuration and prestress effect on SIFs for inclined cracks in steel plates", *Journal of Structural Engineering*, May 1, Vol. 143 No. 5, 04016229, doi: [10.1061/\(asce\)st.1943-541x.0001727](https://doi.org/10.1061/(asce)st.1943-541x.0001727).

-
- El-Sagheer, I., Taimour, M., Mobtasem, M., Abd-Elhady, A. and Sallam, H.E.M. (2020), "Finite Element analysis of the behavior of bonded composite patches repair in aircraft structures", *Frattura Ed Integrità Strutturale*, Sep 23, Vol. 14 No. 54, pp. 128-138, doi: [10.3221/igf-esis.54.09](https://doi.org/10.3221/igf-esis.54.09).
- Equbal, A., Shamim, M., Badruddin, I.A., Equbal, M.I., Sood, A.K., Nik Ghazali, N.N. and Khan, Z.A. (2020), "Application of the combined ANN and GA for multi-response optimization of cutting parameters for the turning of glass fiber-reinforced polymer composites", *Mathematics*, Vol. 8 No. 6, p. 947, doi: [10.3390/math8060947](https://doi.org/10.3390/math8060947).
- Günther, G. and Maier, A. (2010), "Composite repair for metallic aircraft structures development and qualification aspects", in *27th International Congress of the Aeronautical Sciences-ICAS 2010*, Vol. 3, pp. 1882-1894.
- Hosseini-Toudeshky, H., Sadighi, M. and Vojdani, A. (2013), "Effects of curing thermal residual stresses on fatigue crack propagation of aluminum plates repaired by FML patches", *Composite Structures*, Jun 1, Vol. 100, pp. 154-162, doi: [10.1016/j.compstruct.2012.12.052](https://doi.org/10.1016/j.compstruct.2012.12.052).
- Kaddouri, K., Ouinas, D. and Bouiadjra, B.B. (2008), "FE analysis of the behaviour of octagonal bonded composite repair in aircraft structures", *Computational Materials Science*, Oct 1, Vol. 43 No. 4, pp. 1109-1111, doi: [10.1016/j.commatsci.2008.03.003](https://doi.org/10.1016/j.commatsci.2008.03.003).
- Khaleel, G.I., Shaaban, I.G., Elsayed, K.M. and Makhoulf, M.H. (2013), "Strengthening of reinforced concrete slab-column connection subjected to punching shear with FRP systems", *IACSIT International Journal of Engineering and Technology*, December, Vol. 5 No. 6, pp. 657-661, doi: [10.7763/ijet.2013.v5.636](https://doi.org/10.7763/ijet.2013.v5.636), available at: <http://www.ijetch.org/papers/636-EA0025.pdf>
- Khan, S.M. and Essaheb, M. (2017), "Effect of patch thickness on the repair performance of bonded composite repair in cracked aluminum plate", *Materials Today: Proceedings*, Jan 1, Vol. 4 No. 8, pp. 9020-9028, doi: [10.1016/j.matpr.2017.07.255](https://doi.org/10.1016/j.matpr.2017.07.255).
- Kumar, A.M. and Hakeem, S.A. (2000), "Optimum design of symmetric composite patch repair to centre cracked metallic sheet", *Composite Structures*, Jul 1, Vol. 49 No. 3, pp. 285-292, doi: [10.1016/s0263-8223\(00\)00005-2](https://doi.org/10.1016/s0263-8223(00)00005-2).
- Li, C., Zhao, Q., Yuan, J., Hou, Y. and Tie, Y. (2019), "Simulation and experiment on the effect of patch shape on adhesive repair of composite structures", *Journal of Composite Materials*, Dec, Vol. 53 Nos 28-30, pp. 4125-4135, doi: [10.1177/0021998319853033](https://doi.org/10.1177/0021998319853033).
- Madani, K., Touzain, S., Feaugas, X., Benguediab, M. and Ratwani, M. (2009), "Stress distribution in a 2024-T3 aluminum plate with a circular notch, repaired by a graphite/epoxy composite patch", *International Journal of Adhesion and Adhesives*, Apr 1, Vol. 29 No. 3, pp. 225-233, doi: [10.1016/j.ijadhadh.2008.05.004](https://doi.org/10.1016/j.ijadhadh.2008.05.004).
- Makwana, A., Shaikh, A.A. and Bakare, A.K. (2018), "Saikrishna C. 3D numerical investigation of aluminum 2024-T3 plate repaired with asymmetric and symmetric composite patch", *Materials Today: Proceedings*, Jan 1, Vol. 5 No. 11, pp. 23638-23647, doi: [10.1016/j.matpr.2018.10.153](https://doi.org/10.1016/j.matpr.2018.10.153).
- Matta, S., Kolanu, N.R., Chinthapenta, V., Manjunatha, C.M. and Ramji, M. (2019), "Progressive damage analysis of adhesively bonded patch repaired carbon fibre-reinforced polymer specimen under compression involving cohesive zone model", *International Journal of Damage Mechanics*, Nov, Vol. 28 No. 10, pp. 1457-1489, doi: [10.1177/1056789519832062](https://doi.org/10.1177/1056789519832062).
- Mohammadi, S. (2020), "Parametric investigation of one-sided composite patch efficiency for repairing crack in mixed mode considering different thicknesses of the main plate", *Journal of Composite Materials*, Vol. 54 No. 22, pp. 3067-3079, doi: [10.1177/0021998320909535](https://doi.org/10.1177/0021998320909535).
- Mohammed, S.M., Mhamdia, R., Albedah, A., Bouiadjra, B.A., Bouiadjra, B.B. and Benyahia, F. (2021), "Fatigue crack growth in aluminum panels repaired with different shapes of single-sided composite patches", *International Journal of Adhesion and Adhesives*, Vol. 105, 102781, doi: [10.1016/j.ijadhadh.2020.102781](https://doi.org/10.1016/j.ijadhadh.2020.102781).
- Montaser, W.M., Shaaban, I.G., Zaher, A.H., Khan, S.U. and Sayed, M.N. (2022), "Structural behaviour of polystyrene foam lightweight concrete beams strengthened with FRP laminates", *International Journal of Concrete Structures and Materials*, Vol. 16 No. 1, 59, ISSN 1976-0485, doi: [10.1186/s40069-022-00549-1](https://doi.org/10.1186/s40069-022-00549-1).

-
- Okafor, A.C., Singh, N., Enemuoh, U.E. and Rao, S.V. (2005), "Design, analysis and performance of adhesively bonded composite patch repair of cracked aluminum aircraft panels", *Composite Structures*, Nov 1, Vol. 71 No. 2, pp. 258-270, doi: [10.1016/j.compstruct.2005.02.023](https://doi.org/10.1016/j.compstruct.2005.02.023).
- Ouinass, D., Bouiadjra, B.B. and Serier, B. (2007a), "The effects of disbonds on the stress intensity factor of aluminium panels repaired using composite materials", *Composite Structures*, Apr 1, Vol. 78 No. 2, pp. 278-284, doi: [10.1016/j.compstruct.2005.10.012](https://doi.org/10.1016/j.compstruct.2005.10.012).
- Ouinass, D., Bouiadjra, B.B., Serier, B. and SaidBekkouche, M. (2007b), "Comparison of the effectiveness of boron/epoxy and graphite/epoxy patches for repaired cracks emanating from a semicircular notch edge", *Composite Structures*, Oct 1, Vol. 80 No. 4, pp. 514-522, doi: [10.1016/j.compstruct.2006.07.005](https://doi.org/10.1016/j.compstruct.2006.07.005).
- Ramji, M. and Srilakshmi, R. (2012), "Design of composite patch reinforcement applied to mixed-mode cracked panel using finite element analysis", *Journal of Reinforced Plastics and Composites*, Vol. 31 No. 9, pp. 585-595, doi: [10.1177/0731684412440601](https://doi.org/10.1177/0731684412440601).
- Sadek, K., Aour, B., Bachir Bouiadjra, B.A., Fari Bouanani, M. and Khelil, F. (2018), "Analysis of crack propagation by bonded composite for different patch shapes repairs in marine structures: a Numerical Analysis", in *International Journal of Engineering Research in Africa*, Trans Tech Publications, Vol. 35, pp. 175-184, doi: [10.4028/www.scientific.net/jera.35.175](https://doi.org/10.4028/www.scientific.net/jera.35.175).
- Schubbe, J.J. and Mall, S. (1999), "Modeling of cracked thick metallic structure with bonded composite patch repair using three-layer technique", *Composite Structures*, Jun 1, Vol. 45 No. 3, pp. 185-193, doi: [10.1016/s0263-8223\(99\)00025-2](https://doi.org/10.1016/s0263-8223(99)00025-2).
- Shaaban, I.G. and Torkey, A. (2015), "Capacity of reinforced concrete structural elements retrofitted with GFRP under cyclic loading", *Composite Materials in Concrete Construction: Proceedings of the International Seminar held at the University of Dundee*, Scotland, UK, 5-6 September 2002, pp. 213-224, available at: <http://www.icevirtuallibrary.com/doi/abs/10.1680/cmicc.31746.0020>
- Shahin, S. and Farid, T. (2017), "On the effectiveness of composites for repair of pipelines under various combined loading conditions: a computational approach using the cohesive zone method", *Journal of Pressure Vessel Technology*, Vol. 139 No. 2, 021405-1, doi: [10.1115/1.4035081](https://doi.org/10.1115/1.4035081).
- Systèmes Dassault (2014), *ABAQUS 6.14 Analysis User's Manual*, Dassault Systems, Providence, RI.
- Wang, Q.Y. and Pidaparti, R.M. (2002), "Static characteristics and fatigue behavior of composite-repaired aluminum plates", *Composite Structures*, May 1, Vol. 56 No. 2, pp. 151-155, doi: [10.1016/s0263-8223\(01\)00176-3](https://doi.org/10.1016/s0263-8223(01)00176-3).

Further reading

- Abd-Elhady, A.A. and Sallam, H.E. (2017), "Discussion of "fatigue behavior of cracked steel plates strengthened with different CFRP systems and configurations" by hai-tao Wang, gang Wu, and jian-biao jiang", *Journal of Composites for Construction*, Jun 1, Vol. 21 No. 3, 07016004, doi: [10.1061/\(asce\)cc.1943-5614.0000767](https://doi.org/10.1061/(asce)cc.1943-5614.0000767).

Corresponding author

Sultan Mohammed Althahban can be contacted at: smalthahban@jazanu.edu.sa

For instructions on how to order reprints of this article, please visit our website:

www.emeraldgroupublishing.com/licensing/reprints.htm

Or contact us for further details: permissions@emeraldinsight.com